SUPERPOSITION METHOD FOR SEMI-CIRCULAR SURFACE CRACK

G. YAGAWA

Department of Nuclear Engineering, University of Tokyo, Bunkyo-ku, Tokyo, Japan

and

T. NISHIOKA
School of Engineering Science and Mechanics, Georgia Institute of Technology, Atlanta, GA 30332,
U.S.A.

Abstract—This paper is concerned with a superposition method of the analytical and the finite element solutions in determining the stress intensity factors for the embedded circular and the semi-circular surface cracks in three-dimensional bodies. The analytical part in the solution is derived as the product of the solution under the plane strain condition in the plane perpendicular to the crack front line and the power series in the direction of the crack line. Although the total numbers of freedoms in the final stiffness equations are comparatively so small, the accuracies of the results obtained by the present method are found satisfactory.

INTRODUCTION

The importance of knowledge of the surface cracks in plates and shells is well recognized in assessing the integrity of the structural components based on the fracture mechanics. Nevertheless, no exact solution is available for this problem because of mathematical intractability. Because of this, several attempts have been made to obtain approximate solutions using semi-analytical procedures[1-5]. There are some limitations to apply these techniques to complex configurations and loads because of the nature of the procedure. As for the numerical methods, the finite element method has proved to be a very useful tool for solving various problems not only in the two-dimensional fracture mechanics but in the complex three-dimensional cases including the surface crack. Unfortunately, the finite element method still has a disadvantage with regard to computing costs as a very fine mesh is used around the crack tip or the crack front line. The cost problem is serious especially in the three-dimensional cases. Several techniques have been reported to overcome this difficulty in the finite element crack analyses and complete surveys are given in[6-8]. Among others, Rashid and Gilman[9], Hellen and Blackburn[10], Broekhoven[11] and Aamods and Klem[12] have utilized the finite element techniques combined with the energy release rates methods in obtaining the stress intensity factors for the surface cracks. Pian and Moriya[13], Hilton *et al.*[14] and Atluri and Kathiresan[15] have solved the same problem by using the enriched crack front elements, respectively. Yagawa *et al.*[16] have employed the discretization error technique of the finite element method in solving the same problem.

The present authors have proposed a superposition method, in which the nodal displacements of the conventional finite element method together with the unknown constants of the analytical solution, are determined in the variational principle. The method has been successfully applied to the two-dimensional as well as the plate bending problems in the fracture mechanics[17, 18]. The purpose of the present study is to show the applicability of the superposition method to the determination of the stress intensity factor of the three-dimensional body with a surface crack.

THEORETICAL BACKGROUND

The superposition method
We consider the three-dimensional body V, where the body is, tentatively, split into two parts $V^{(0)}$ and $V^{(1)}$ which are assumed to be contiguous on $S^{(01)}$ (Fig. 1). The potential energy
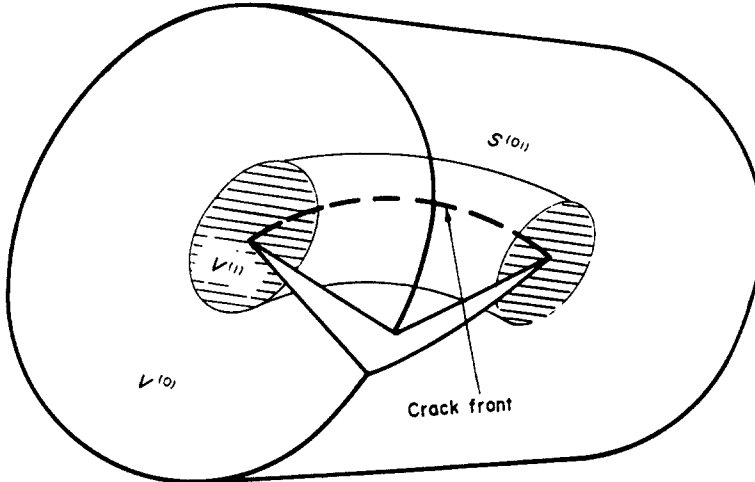
Fig. 1. Cracked body split fictitiously into two parts.

functional in this case can be modified as follows[19]

$$\pi_I = \sum_{\alpha=0}^{1} \left(\frac{1}{2} \int_{V^{(\alpha)}} \sigma_{ij}^{(\alpha)} \epsilon_{ij}^{(\alpha)} \, dV - \int_{S_\sigma^{(\alpha)}} \bar{T}_i^{(\alpha)} u_i^{(\alpha)} \, dS \right)$$

$$- \int_{S^{(01)}} \lambda_i (u_i^{(0)} - u_i^{(1)}) \, dS \tag{1}$$

where the continuity conditions on $S^{(01)}$ are incorporated. Here, σ_{ij}, ϵ_{ij} and u_i are stresses, strains and displacements, respectively. λ_i are Lagrange multipliers defined on $S^{(01)}$. S_σ is the part of the surface S of the body V in which the prescribed traction $\bar{T}_i$ is given. ( )$^{(\alpha)}$, $\alpha = 0$ and 1, denote the variables corresponding to $V^{(\alpha)}$, $\alpha = 0$ and 1, respectively.

Introducing the physical meaning of λ_i in eqn (1), we have the alternative forms as follows

$$\pi_{II} = \sum_{\alpha=0}^{1} \left(\frac{1}{2} \int_{V^{(\alpha)}} \sigma_{ij}^{(\alpha)} \epsilon_{ij}^{(\alpha)} \, dV - \int_{S_\sigma^{(\alpha)}} \bar{T}_i^{(\alpha)} u_i^{(\alpha)} \, dS \right)$$

$$- \int_{S^{(01)}} T_i^{(1)} (u_i^{(1)} - u_i^{(0)}) \, dS \tag{2}$$

$$\pi_{III} = \sum_{\alpha=0}^{1} \left(\frac{1}{2} \int_{V^{(\alpha)}} \sigma_{ij}^{(\alpha)} \epsilon_{ij}^{(\alpha)} \, dV - \int_{S_\sigma^{(\alpha)}} \bar{T}_i^{(\alpha)} u_i^{(\alpha)} \, dS \right)$$

$$- \int_{S^{(01)}} (T_i^{(0)} (u_i^{(0)} - u_i^{(1)}) \, dS. \tag{3}$$

In this paper, eqn (3) is adopted as the variational principle.

Next, we show the superposition method based on the finite element model and the analytical solution for augmentation. The displacements $u_i^{(0)}$ and $u_i^{(1)}$ in this method can be written as follows

$$u_i^{(0)} = \hat{u}_i^{(0)} \qquad \text{in } V^{(0)} \tag{4}$$

$$u_i^{(1)} = \hat{u}_i^{(1)} + \bar{u}_i \qquad \text{in } V^{(1)} \tag{5}$$

where $\hat{u}_i^{(0)}$ and $\hat{u}_i^{(1)}$ are the usual finite element displacements which are, respectively, written as

$$\hat{u}_i^{(\alpha)} = N_{im} d_m^{(\alpha)}, \qquad \alpha = 0 \text{ and } 1 \tag{6}$$

Here, N_{im} are the interpolation functions and the nodal displacements $d_m^{(0)}$ and $d_m^{(1)}$ in $V^{(0)}$ and $V^{(1)}$, respectively, are defined independently on $S^{(01)}$. On the other hand, $\bar{u}_i$ in eqn (5) are the

analytical solutions which can be written as

$$\bar{u}_i = Q_{im}\bar{d}_m.$$ (7)

Here, Q_{im} are the shape functions and $\bar{d}_m$ are the generalized coordinates.

The stresses and the strains are calculated from the usual relations

$$\sigma_{ij}^{(\alpha)} = D_{ijkl}\epsilon_{kl}^{(\alpha)}, \qquad \alpha = 0 \text{ and } 1$$ (8)

$$\epsilon_{kl}^{(\alpha)} = \frac{1}{2}(u_{i,j}^{(\alpha)} + u_{j,i}^{(\alpha)}), \qquad \alpha = 0 \text{ and } 1$$ (9)

where D_{ijkl} are the elastic modulus tensors.

The traction forces $T_i^{(0)}$ are obtained from the relation

$$T_i^{(0)} = \sigma_{ij}^{(0)} n_j^{(0)}$$ (10)

where $n_j^{(0)}$ are the unit normals on $S^{(01)}$ drawn outwards from the domain $V^{(0)}$.

Introducing eqns (4) and (5) together with eqns (6) and (7) into eqns (8)–(10) and expressing eqn (3) as a function of the nodal displacements $d_m^{(\alpha)}$, $\alpha = 0$ and 1, and the generalized coordinates $\bar{d}_m$ leads, with the variation of eqn (3), to the following matrix equation

$$\begin{bmatrix} \mathbf{K}^{(00)} & \mathbf{K}^{(01)} & \mathbf{K}^{(0A)} \\ & \mathbf{K}^{(11)} & \mathbf{K}^{(1A)} \\ \text{sym.} & & \mathbf{K}^{(AA)} \end{bmatrix} \begin{Bmatrix} \mathbf{d}^{(0)} \\ \mathbf{d}^{(1)} \\ \bar{\mathbf{d}} \end{Bmatrix} = \begin{Bmatrix} \mathbf{P}^{(0)} \\ \mathbf{P}^{(1)} \\ \bar{\mathbf{P}} \end{Bmatrix}$$ (11)

from which the nodal displacements of the finite elements and the generalized coordinates of the analytical solutions are directly obtained. The details of eqn (11) are given in the Appendix.

Analytical solutions for circular crack

Figure 2 shows the circular crack and its coordinates. The crack is located in the $x - y$ plane with 0 being the crack center and z-axis is perpendicular to the crack surface. S denotes the length along the crack front line measured from the y-axis. The polar coordinates (ρ, φ) are defined the $x - y$ plane as

$$\rho = \sqrt{(x^2 + y^2)}$$ (12a)

$$\varphi = \tan^{-1}(y/x).$$ (12b)

In addition, the polar coordinates (r, θ) are defined in the $\rho - z$ plane as

$$r = \sqrt{((\rho - a)^2 + z^2)}$$ (13a)

$$\theta = \tan^{-1}(z/(\rho - \rho_0))$$ (13b)
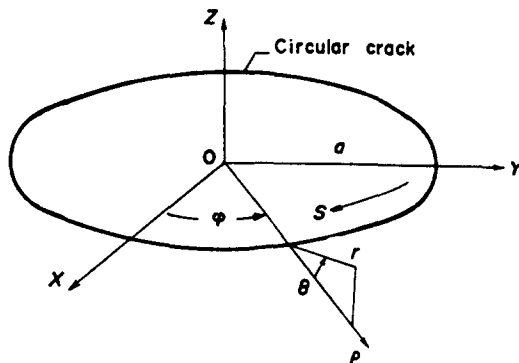
where a is the radius of crack.

Fig. 2. Circular crack and its coordinates.

It is well known that the plane strain condition holds in the $\rho - z$ plane when r tends to zero. This is violated if the crack front line approaches the free surface. In this paper, however, we consider that the solutions based on the plane strain condition can be applied even near the cross point of the crack line and the free surface since the special region where the plane strain condition is unvalidated is limited to very small part of the crack and can be disregarded from the practical point of view[20].

From the above consideration, the analytical displacements can be written as follows

$$\bar{u}_\rho = f(s)\hat{u}_\rho(r, \theta) \tag{14a}$$

$$\bar{u}_z = f(s)\hat{u}_z(r, \theta) \tag{14b}$$

$$\bar{u}_\varphi = g(s)\hat{u}_\varphi(r, \theta) \tag{14c}$$

where the functions $f(s)$ and $g(s)$ are approximated using the power series as

$$f(s) = \sum_{m=0}^{M_s-1} a_m s^m \tag{15a}$$

$$g(s) = \sum_{m=0}^{M_s-1} b_m s^m \tag{15b}$$

where a_m and b_m, $m = 0, 1, \ldots$, are the unknown parameters and M_s denotes the number of terms employed in the series.

On the other hand, the functions $\hat{u}_\rho(r, \theta)$, $\hat{u}_z(r, \theta)$ and $\hat{u}_\varphi(r, \theta)$ in eqns (14) can be written as follows[21]

$$\hat{u}_\rho(r, \theta) = \hat{u}_{\rho I}(r, \theta) + \hat{u}_{\rho II}(r, \theta) \tag{16a}$$

$$\hat{u}_z(r, \theta) = \hat{u}_{zI}(r, \theta) + \hat{u}_{zII}(r, \theta) \tag{16b}$$

$$\hat{u}_\varphi(r, \theta) = \hat{u}_{\varphi III}(r, \theta) \tag{16c}$$

where

$$\hat{u}_{\rho I}(r, \theta) = \sum_{n=0}^{M_r-1} \frac{\sqrt{(2a)}}{8G} c_{In} r^{n+(1/2)} h_{\rho I}(n, \theta, \nu) \tag{17a}$$

$$\hat{u}_{zI}(r, \theta) = \sum_{n=0}^{M_r-1} \frac{\sqrt{(2a)}}{8G} c_{In} r^{n+(1/2)} h_{zI}(n, \theta, \nu) \tag{17b}$$

$$\hat{u}_{\rho II}(r, \theta) = \sum_{n=0}^{M_r-1} \frac{\sqrt{(2a)}}{8G} c_{IIn} r^{n+(1/2)} h_{\rho II}(n, \theta, \nu) \tag{17c}$$

$$\hat{u}_{zII}(r, \theta) = \sum_{n=0}^{M_r-1} \frac{\sqrt{(2a)}}{8G} c_{IIn} r^{n+(1/2)} h_{zII}(n, \theta, \nu) \tag{17d}$$

$$\hat{u}_{\varphi III}(R, \theta) = \sum_{n=0}^{M_r-1} \frac{\sqrt{(2a)}}{8G} c_{IIIn} r^{n+(1/2)} h_{\varphi III}(n, \theta, \nu). \tag{17e}$$

Here, $h_{\rho I}(n, \theta, \nu), \cdots$ are appropriate functions of n, θ and ν, G is the shear modulus, ν is the Poisson's ratio, c_{In}, c_{IIn}, c_{IIIn}, $n = 0, 1, \cdots$, are unknown parameters and $( )_I$, $( )_{II}$ and $( )_{III}$ correspond to the crack opening modes I, II and III, respectively. M_r is the number of terms employed in the series. In eqns (17), the terms of r^n, $n = 0, 1, \cdots$, are not included because the finite element displacements of the quadratic isoparametric elements can replace these terms with enough accuracy.

The analytical strains in the cylindrical coordinates (ρ, φ, z) are given using eqns (14) as follows

$$\bar{\epsilon}_{\rho\rho} = f(s)\frac{\partial \hat{u}_\rho}{\partial \rho} \tag{18a}$$

$$\bar{\varepsilon}_{zz} = f(s)\frac{\partial \hat{u}_z}{\partial z} \tag{18b}$$

$$\bar{\varepsilon}_{\varphi\varphi} = \frac{g'(s)}{\rho}\hat{u}_\varphi + \frac{f(s)}{\rho}\hat{u}_\rho \tag{18c}$$

$$\bar{\varepsilon}_{\rho z} = \frac{f(s)}{2}\left(\frac{\partial \hat{u}_\rho}{\partial z} + \frac{\partial \hat{u}_z}{\partial \rho}\right) \tag{18d}$$

$$\bar{\varepsilon}_{\rho\varphi} = \frac{1}{2}\left(\frac{f'(s)}{\rho}\hat{u}_\rho + g(s)\frac{\partial \hat{u}_\rho}{\partial \rho} - \frac{g(s)}{\rho}\hat{u}_\rho\right) \tag{18e}$$

$$\bar{\varepsilon}_{z\varphi} = \frac{1}{2}\left(g(s)\frac{\partial \hat{u}_\varphi}{\partial z} + \frac{f'(s)}{\rho}\hat{u}_z\right) \tag{18f}$$

where

$$f'(s) = \frac{df(s)}{ds}\frac{ds}{d\varphi} \tag{19a}$$

$$g'(s) = \frac{dg(s)}{ds}\frac{ds}{d\varphi}. \tag{19b}$$

Combining the unknown parameters in eqns (15) with those in eqns (17), we define the new unknown parameters e_{Imn}, e_{IImn} and e_{IIImn}, $m, n = 0, 1, \cdots$, as follows

$$e_{Imn} = a_m c_{In} \tag{20a}$$

$$e_{IImn} = a_m c_{IIn} \tag{20b}$$

$$e_{IIImn} = a_m c_{IIIn} \tag{20c}$$

$$m = 0, 1, \cdots, (M_s - 1)$$

$$n = 0, 1, \cdots, (M_r - 1).$$

Thus, the generalized coordinates in eqn (7) can be expressed in terms of eqns (20) as follows

$$\bar{d} = [e_{I00}, e_{I10}, \cdots, e_{I(M_s-1)0}, \cdots, e_{I(M_s-1)(M_r-1)},$$

$$e_{II00}, e_{II10}, \cdots, e_{II(M_s-1)0}, \cdots, e_{II(M_s-1)(M_r-1)},$$

$$e_{III00}, e_{III10}, \cdots, e_{III(M_s-1)0}, \cdots, e_{III(M_s-1)(M_r-1)}]^T \tag{21}$$

As for the finite elements, we use the 20-noded isoparametric elements[22], which are suitable for the curved geometries such as the surface cracks. The superposition of the analytical solutions on the finite elements is made in the orthogonal Cartesian coordinates (x, y, z) after converting the coordinates of the finite elements from the cylindrical ones to the orthogonal Cartesian ones.

Following the above procedure, the stiffness matrix and the load vector in eqn (11) are determined as usual. Solving this equation for $\bar{d}$, we can obtain the stress intensity factors as follows

$$K_I(s) = \sqrt{(\pi a)}\sum_{m=0}^{M_s-1} e_{Im0}s^m \tag{22a}$$

$$K_{II(s)} = \sqrt{(\pi a)}\sum_{m=0}^{M_s-1} e_{IIm0}s^m \tag{22b}$$

$$K_{III(s)} = \sqrt{(\pi a)}\sum_{m=0}^{M_s-1} e_{IIIm0}s^m. \tag{22c}$$

RESULTS

Circular crack in round bar subject to tension

In order to show the validity of the present method, the analysis is made for a circular crack

in round bar under uniform tension σ_0 at the ends (Fig. 3). The radius and the length of the bar are, respectively, R and $2L$, and the radius of the crack is a. Although this problem can be solved with the axisymmetric treatment, we employ rather the three-dimensional technique mentioned above. From the symmetry of the structure, one eighth of the bar is analysed as shown in Fig. 4, where the shaded region and the rest of the structure are, respectively, corresponding to $V^{(1)}$ and $V^{(0)}$. The total number of elements is 14 and that of nodal points is 159. Moreover, the numbers of terms in the analytical solutions M_r and M_s are 2 and 1, respectively. Figure 5 shows the normalized stress intensity factors versus the ratio a/R. It can be seen from the figure that the present solution is favorably compared with the other solutions in the two-dimensional regime[23, 24].

Semi-circular surface crack in block subject to tension

Next example is the analysis of the stress intensity factor for a block with a semi-circular surface crack which is subject to uniform tensile stress σ_0 at the ends (Fig. 6). The width, the length and the thickness of the block are $2W$, $2L$ and H, respectively. The radius of the crack is a. Figure 7 shows the mesh subdivision for one quarter of the block taking advantage of the symmetry of the structure. As seen from the comparison between Figs. 4 and 7, both mesh arrangements are taken to be the same. The one of the number of terms in the analytical solutions M_r is set to be 2, and the other M_s is parametrically changed from 2 to 5. Figure 8 shows the distributions of the nondimensional stress intensity factors along the crack front line for the case of $a/W = 0.5$, $a/H = 0.5$ and $L/W = 3.0$. As can be seen from the top of the figure which shows the error from the results with $M_s = 5$, the discrepancies in the stress intensity factors with M_s being greater than 3 from the value with M_s being 5 are less than 1% throughout the crack frontline. Similarly, Fig. 9 shows the case of $a/W = 0.2$, $a/H = 0.2$ and $L/W = 3.0$. The difference of the solutions between $M_s = 4$ and 5 in this case is less than 2%, and our results are compared in good agreement with those
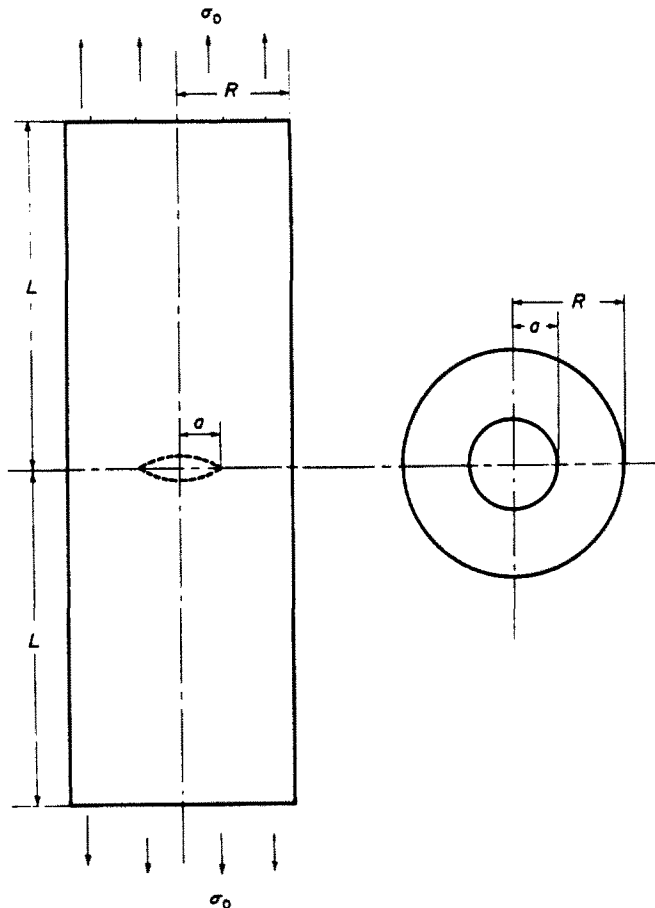

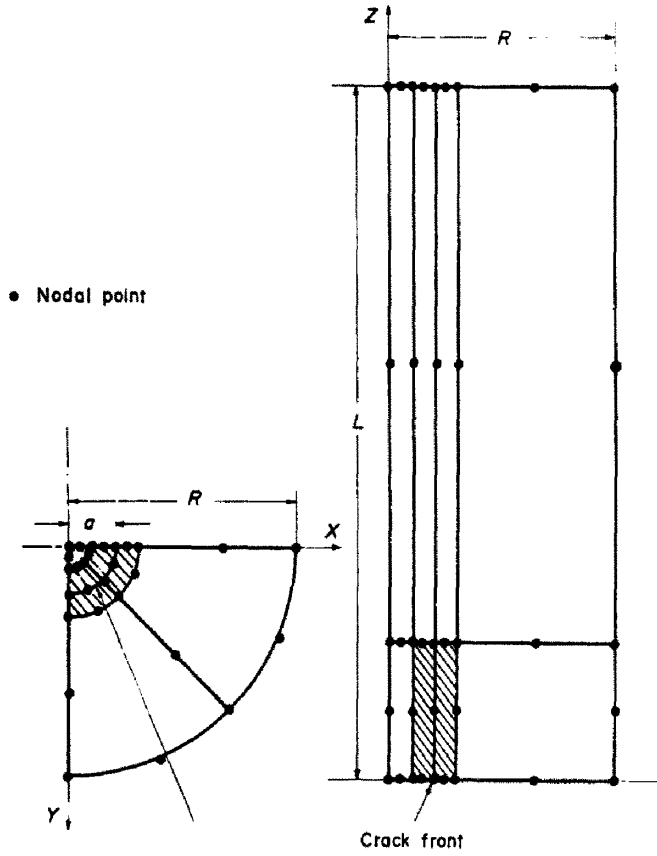Fig. 3. Circular crack in round bar under uniform tension.

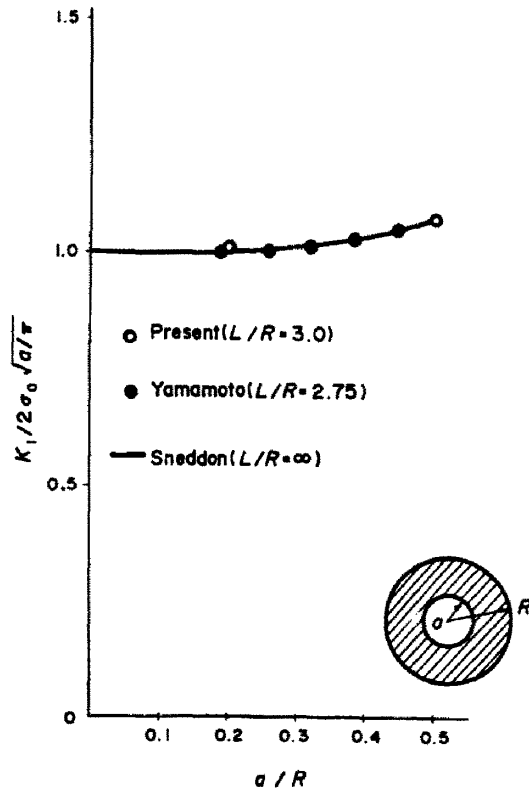Fig. 4. Mesh subdivision for one eighth of the bar with a crack.

Fig. 5. Normalized stress intensity factors vs the ratio a/R ($M_r = 2, M_s = 1$).
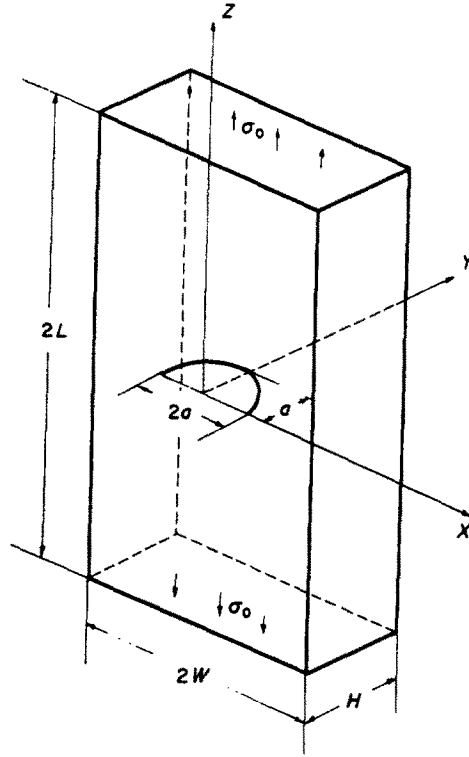
Fig. 6. Semi-circular surface crack in block under uniform tension.
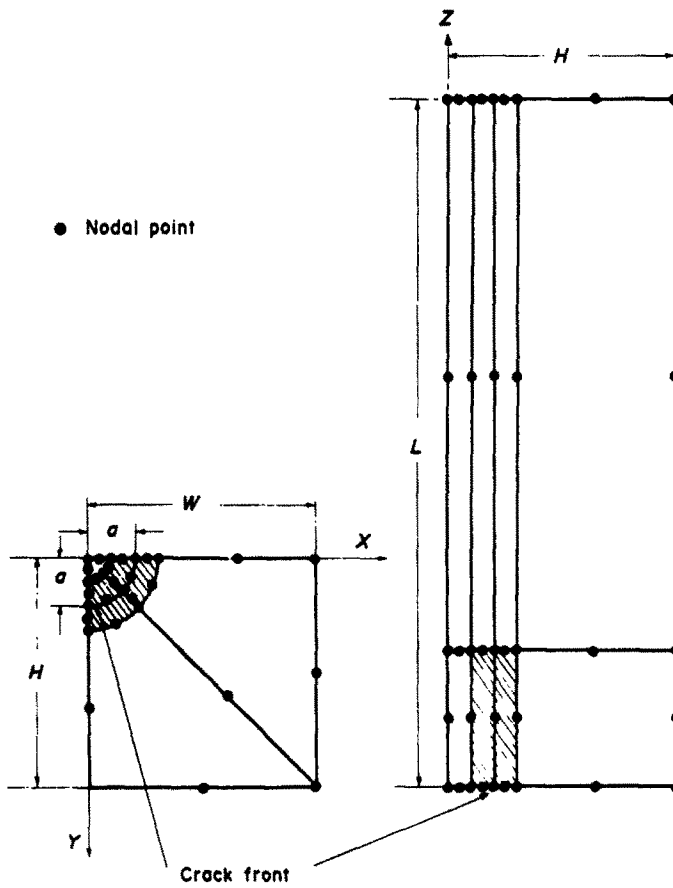

● Nodal point

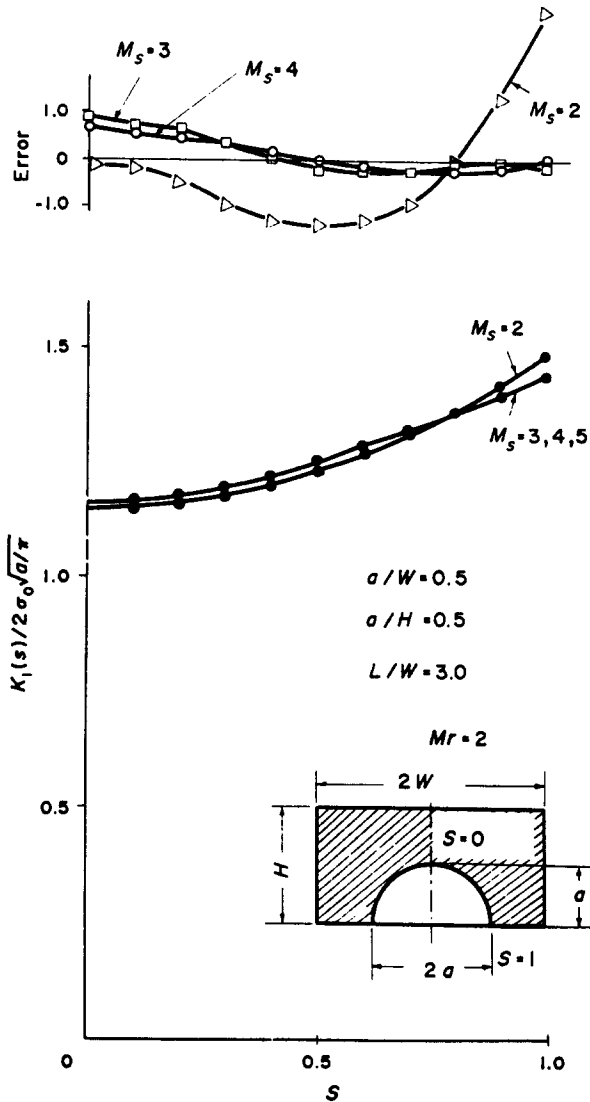Fig. 7. Mesh subdivision for one quarter of the block with a crack.

Fig. 8. Distributions of the normalized stress intensity factors along the crack front line $(a/W = a/H = 0.5, L/W = 3.0; M_r = 2)$.

by Tracey[25] with the same geometry but $L/W = 1.0$ using the special crack tip elements, in which the total numbers of isoparametric elements (8-node) and the nodal points are, respectively, 486 and 587.

Finally, it should be noted on the evaluations of $K^{(1A)}$ and $K^{(AA)}$ which contain singularity at the crack front line that the special integration technique is used in the $\rho - z$ plane by applying the least squares methods to the results obtained by the Legendre-Gauss quadrature, and the usual 3 and 5 points Legendre-Gauss quadratures are used, respectively, in the φ-direction for the circular crack in the round bar and the semi-circular surface crack in the block.

CONCLUSIONS

The superposition method of the analytical and the finite element solutions is applied to the evaluations of the three-dimensional stress intensity factors for a circular crack in a bar and for a semi-circular surface crack in a block both under uniform tensions. From the numerical experiments given in this paper, we could conclude that the present method is accurate and economical comparatively due to the small degree of freedoms in the final equation.

Concerning the singularity problem near the point where a crack front line intersects the surface of a body[26], we have not considered this effect in our calculations although the method has potential to treat the problem. According to the analysis of through wall crack[20], the stress intensity factor decreases rapidly near the surface and the relevant region is limited
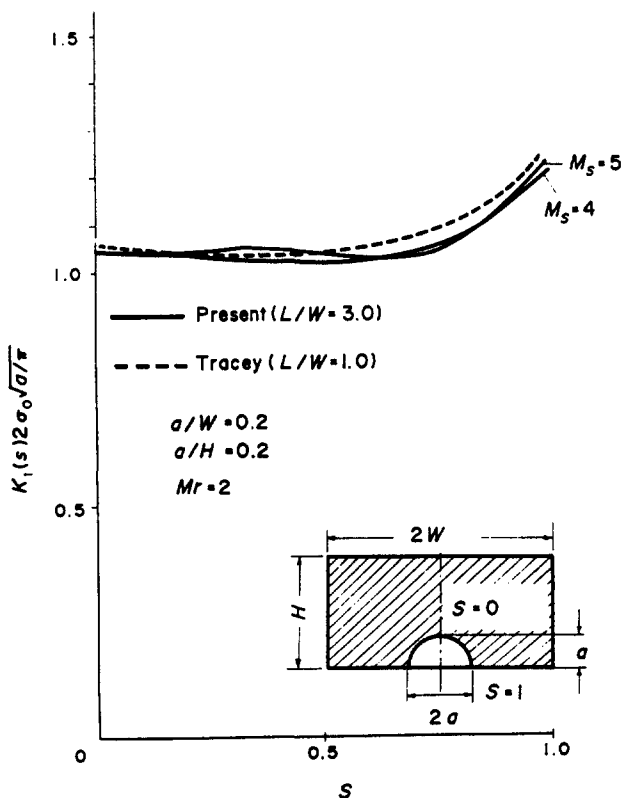
Fig. 9. Distributions of the normalized stress intensity factors along the crack front line $(a/W = a/H = 0.2; M_r = 2)$.

only to 0.5% of the plate thickness. This means that, at least practically, the effect could be neglected in the calculation.

REFERENCES

1. G. R. Irvin, Crack extension force for a part-through crack in a plate. *J. Appl. Mech.* **29**, *Trans.* ASME, Series E, 651–654 (1962).
2. R. C. Shah and A. S. Kobayashi, On the surface flaw problem. *The Surface Crack: Physical Problems and Computational Solutions* (Edited by J. L. Swedlow) pp. 79–124 ASME (1972).
3. F. W. Smith, The elastic analysis of the part-circular surface flaw problem by the alternating method. *The Surface Crack: Physical Problems and Computational Solutions* (Edited by J. L. Swedlow) pp. 125–152. ASME (1972).
4. T. A. Cruse, Numerical evaluation of elastic stress intensity factors by the boundary-integral equation method. *The Surface Crack: Physical Problems and Computational Solutions* (Edited by J. L. Swedlow) pp. 153–170. ASME (1972).
5. J. R. Rice and N. Levy, The part-through surface crack in an elastic plate. *J. Appl. Mech.* **39**, *Trans.* ASME, Series E, pp. 185–194. ASME, Series E, (1972).
6. R. H. Gallagher, A review of finite element techniques in fracture mechanics. *Proc. 1st Int. Conf. on Numerical Methods in Fracture Mechanics* (Edited by A. R. Luxmoore and D. R. J. Owen, pp. 1–25. University College Swansea, Swansea, United Kingdom (1978).
7. M. C. Apostal, S. Jordan and P. V. Marca, *The finite element techniques for posturated flaws in shell structures*. EPRI-SR-22, Electric Power Research Institute, Palo Alto, Ca. (1975).
8. Y. Ando and G. Yagawa, Recent developments in finite element method of three-dimensional crack problems in Japan. *Proc. Int. Conf. Fracture Mechanics and Tech.* (Edited by G. C. Sih and C. L. Chow), pp. 1513–1528. Sijthoff and Noordhoff (1977).
9. Y. R. Rashid and J. D. Gilman, Three-dimensional analysis of reactor pressure vessel nozzles. *First Int. Conf. on Structural Mechanics in Reactor Technology*, Berlin, Paper G2/6 (1971).
10. T. K. Hellen, and W. S. Blackburn, The calculation of stress intensity factors in two and three-dimensions using finite elements. *Computational Fracture Mechanics* (Edited by E. F. Rybicki and S. E. Benzley) pp. 103–120. ASME (1975).
11. M. J. B. Broekhoven, *Theoretical and Experimental Analysis of Crack Extension at Nozzle Junction*, pp. 535–558. ASTM STP 601 (1976).
12. B. Aamods and F. Klem, Application of numerical techniques in practical fracture mechanics. *Fracture Mechanics in Engineering Practice* (Edited by P. Stanley) pp. 33–56. Applied Science London (1977).
13. T. H. H. Pian and K. Moriya, Three-dimensional fracture analysis by assumed stress hybrid elements. *Proc. 1st Int. Conf. on Numerical Methods in Fracture Mech.* (Edited by A. R. Luxmoore and D. R. J. Owen) pp. 363–373. University College Swansea, Swansea, United Kingdom (1978).
14. P. D. Hilton, B. V. Kiefer and G. C. Sih, Specialized finite element procedures for three-dimensional crack problems. *Proc. 1st Int. Conf. on Numerical Methods in Fracture Mech.* (Edited by A. R. Luxmoore and D. R. J. Owen), pp. 411–421. University College Swansea, Swansea, United Kingdom (1978).
15. S. N. Atluri and K. Kathiresan, 3D analyses of surface flaws in thick-walled reactor pressure-vessels using displacement-hybrid finite element method. *Nuclear Engineering and Design*, **51**, 163–176 (1979).

16. G. Yagawa, M. Ichimiya and Y. Ando, Two and three-dimensional analyses of stress intensity factors based on discretization error in finite elements. *Proc. 1st Int. Conf. on Numerical Methods in Fracture Mech.* (Edited by A. R. Luxmoore and D. R. J. Owen), pp. 249-267. University College Swansea, Swansea, United Kingdom (1978).
17. G. Yagawa, T. Nishioka, Y. Ando and N. Ogura, The finite element calculation of stress intensity factors using superposition. *Computational Fracture Mechanics* (Edited by E. F. Rybicki and S. E. Benzley) pp. 21-34, ASME (1975).
18. G. Yagawa and T. Nishioka, Finite element analysis of stress intensity factors for plane extension and plate bending problems. *Int. J. Numerical Methods in Engineering.* Vol. 14, 727-740 (1979).
19. K. Washizu, *Variational Methods in Elasticity and Plasticity,* 2nd Edn, Pergamon Press, England (1975).
20. Y. Yamamoto and Y. Sumi, Stress intensity factor for three-dimensionas cracks. *Int. J. Fracture,* Vol. 14. 17-38 (1978).
21. N. Muskhelishivili, *Some Basic Problems of the Mathematical Theory of Elasticity,* 4th Edn. Noordhoff, Leyden (1963).
22. O. C. Zienkiewicz, *The Finite Element Method in Engineering Science.* McGraw-Hill, New York (1971).
23. I. N. Sneddon, The distribution of stress in the neighborhood of a crack in an elastic solid. *Proc. R. Soc.* (London). Series A, 187, 229-260 (1946).
24. Y. Yamamoto, N. Tokuda and Y. Sumi, Finite element treatment of singularities of boundary value problems and its application to analysis of stress intensity factors. *Theory and Practice in Finite Element Structural Analysis* (Edited by Y. Yamada, and R. H. Gallagher) pp. 75-90, University of Tokyo Press (1973).
25. D. M. Tracey, 3-D elastic singularity element for evaluation of K along an arbitrary crack front. *Int. J. Fracture Mech.* Vol. 9, 340-343 (1973).
26. J. P. Benthem, *Three-dimensional state of stress at the vertex of a quater-infinite crack in a half-space.* Rep. No. 563, Laboratory of Engineering Mechanics, Delft University of Technology (1975).

APPENDIX

$$K_{pq}^{(00)} = \int_{V^{(0)}} D_{ijkl} N_{ip,j}^{(0)} N_{kq,l}^{(0)} \, dV - \int_{S^{(01)}} D_{ijkl} (N_{ip}^{(0)} N_{kq,l}^{(0)}$$

$$+ N_{kp,l}^{(0)} N_{iq}^{(0)}) n_j^{(0)} \, dS$$

$$K_{pq}^{(01)} = \int_{S^{(01)}} D_{ijkl} N_{kp,l}^{(0)} N_{iq}^{(1)} n_j^{(0)} \, dS$$

$$K_{pq}^{(0A)} = \int_{S^{(01)}} D_{ijkl} N_{kp,l}^{(0)} Q_{iq} n_j^{(0)} \, dS$$

$$K_{pq}^{(11)} = \int_{V^{(1)}} D_{ijkl} N_{ip,j}^{(1)} N_{kq,l}^{(1)} \, dV$$

$$K_{pq}^{(1A)} = \int_{V^{(1)}} D_{ijkl} N_{ip,j}^{(1)} Q_{kq,l} \, dV$$

$$K_{pq}^{(AA)} = \int_{V^{(1)}} D_{ijkl} Q_{ip,j} Q_{kq,l} \, dV$$

$$P_p^{(0)} = \int_{S_\sigma^{(0)}} \bar{T}_i^{(0)} N_{ip}^{(0)} \, dS$$

$$P_p^{(1)} = \int_{S_\sigma^{(1)}} \bar{T}_i^{(1)} N_{ip}^{(1)} \, dS$$

$$P_p^{(A)} = \int_{S_\sigma^{(1)}} \bar{T}_i^{(1)} Q_{ip} \, dS.$$